Journal of Glaciology, Vol. 40, No. 135, 1994

Observations of flexural waves on the Erebus Ice Tongue, McMurdo Sound, Antarctica, and nearby sea ice

VERNON A. SQUIRE,
Department of Mathematics and Statistics, University of Otago, Dunedin, New Zealand

WILLIAM H. ROBINSON,
New Zealand Institute for Industrial Research and Development, Lower Hutt, Wellington, New Zealand

MICHAEL MEYLAN,
Department of Mathematics and Statistics, University of Otago, Dunedin, New Zealand

TIMOTHY G. HASKELL
New Zealand Institute for Industrial Research and Development, Lower Hutt, Wellington, New Zealand

ABSTRACT. New strain data relating to flexural oscillations of the Erebus Glacier Tongue (EGT), McMurdo Sound, Antarctica, are presented and are analysed in the frequency domain. The data were collected during November 1989, just 3 months prior to the most recent calving of the ice tongue which occurred in March 1990. A broad-band oscillation centred on 50 s is found in both the strain measurements collected on the EGT and those collected on the sea ice nearby. The oscillation is shown, at least in part, to be propagating with a phase velocity of approximately 65 m s^{-1} in a direction away from the snout towards the grounding line, rather than being wholly due to a standing-wave pattern in the EGT. A coupling model between the sea ice and the EGT is proposed and is shown to compare reasonably well with the data.

INTRODUCTION

The Erebus Glacier Tongue (EGT) flows from the western side of Mount Erebus into McMurdo Sound, about 20 km north of New Zealand's Scott Base and the nearby United States base, McMurdo (Fig. 1). Its close proximity to excellent logistical support has meant that the EGT has been the focus of a number of experimental and theoretical studies to map its geometry and structure (Holdsworth, 1982), and to understand its dynamics (Holdsworth, 1969, 1974; Goodman and Holdsworth, 1978; Holdsworth and Holdsworth, 1978; Holdsworth and Glynn, 1981; Vinogradov and Holdsworth, 1985; Gui and Squire, 1989).

The EGT is known to have calved at least three times since the turn of the century: in March 1911 members of Scott's British Antarctic (*Terra Nova*) Expedition observed a major calving event and the formation of an approximately 4 km^2 tabular iceberg weighing more than 100×10^6 tonnes; a similar calving was deduced by Holdsworth (1974) to have occurred in the 1940s and he suggested another calving was imminent. The last calving occurred on 1 March 1990 (Robinson and Haskell, 1990), 3 months after the measurements that are reported in this paper were collected.

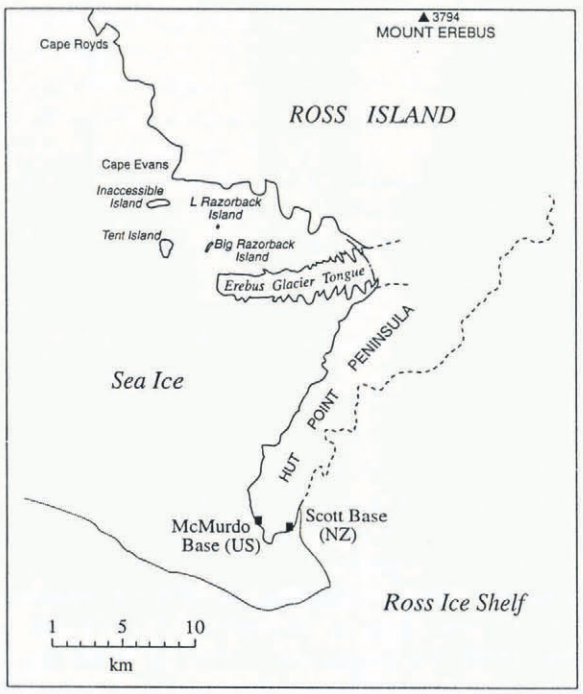

Fig. 1. Map showing Erebus Glacier Tongue in relation to New Zealand's Scott Base and the U.S. McMurdo Station.

https://doi.org/10.3189/S0022143000007462 Published online by Cambridge University Press

These calvings and many others in similar ice tongues took place at some distance from the grounding line, where one might expect the bending moments and stresses to be largest. This has led to the suggestion that the calving is due to the build-up of standing waves in the tongue and that these are of sufficient amplitude to produce fatigue failure of the ice after many cycles. All theoretical studies have assumed that the waves are standing. Various groups have measured strain or tilt on the EGT (e.g. Goodman and Holdsworth, 1978; Holdsworth and Holdsworth, 1978) and have attributed the observed oscillations in strain to standing flexural waves.

In 1984, the New Zealand Department of Scientific and Industrial Research (DSIR) Physical Sciences buried sensitive strain gauges in the EGT to monitor oscillations and to observe a calving event, noting that one was overdue. Strains were measured daily from October 1984 to 1989, and were telemetered to Scott Base where they were recorded on floppy disk. Initially, two strain gauges were buried lengthways either side of the tongue, 3.5 km from the snout. The strains from these two instruments were in phase and of similar amplitudes, which is consistent with a lengthwise flexure of the tongue (Robinson and Haskell, 1992). A rosette of three strain gauges was used to investigate further the mode of vibration. The major principal strain was found to lie along the length of the tongue and the minor principal strain was found to be approximately $-\frac{1}{3}$ of the major principal strain (Robinson and Haskell, 1992). This was additional evidence that the strains were due to lengthwise flexure of the ice tongue. Since, at this time, it was not possible to distinguish between standing and travelling waves, two more strain gauges were placed at distances of 180 and 1700 m towards the snout. Results from the three strain gauges suggested that flexural waves were travelling from the snout towards the grounding line at a phase speed of approximately $70 \pm 10\,\mathrm{m\,s^{-1}}$ (Robinson and Haskell, 1992).

To clarify further these observations, which were quite sparse, the present intensive study was staged during November 1989. It is the analysis of these 1989 data that is the subject of this paper. The long data set telemetered from Scott Base during 1984–89 is deficient in several respects, mainly because of limitations in the band width of the telemetry system. The 1984–89 data set cannot, for example, be used for spectral analysis because the length of the data records transmitted is too short for meaningful statistical interpretation. It was intended for, and is therefore more suited to, climatological work; for instance, looking for long-term changes preceding a calving event. The November 1989 experiment, on the other hand, only took place over a few days but the records were collected with the aim of interpreting the data fully. Unfortunately, the long-awaited EGT calving event of March 1990 took place after all the DSIR strain gauges had been uplifted.

The most recent measurements of the dimensions of the EGT were made in December 1985 (DeLisle and others, 1989). Its length was 15 km, of which the last 13.5 km were floating, and its thickness varied from 50 m at the snout to 300 m at the grounding line. Its width varied from 0.5 to 2 km with many large bays along its sides. The depth of McMurdo Sound is about 300 m at the EGT's snout. The EGT grows at the rate of about 150 m year^{-1} (DeLisle and others, 1989). Most of the year it is surrounded by sea ice of 1–3 m thickness and it is only for a short time at the height of summer that the sea ice melts around the tongue (Robinson and Haskell, 1992).

The results of Robinson and Haskell (1992) suggest that the strains in the EGT are due to length-wise flexural waves, and in the rest of this paper we shall assume that this is the case.

FLEXURAL WAVES

A commonly used model for a floating ice sheet which is flexing under the action of small-amplitude waves is that of a perfectly elastic, thin plate on a fluid foundation. The alternative use of a thick-plate model, which includes the effect of rotatory inertia and transverse shear, has been investigated by Fox and Squire (1991a) and it has been shown to be unnecessary except in the case of very short waves or very thick ice. For example, Fox and Squire (1991a) found the thin- and thick-plate models agreed for periods greater than 20 s with 200 m thick ice. Thus, the present geometries for either the EGT or the sea ice of McMurdo Sound do not call for this more complicated theory; a thin-plate theory is quite adequate.

The ice-plate model and dispersion relation

The dispersion relation for a thin sea-ice plate of thickness h and density ρ' is derived by assuming an homogeneous ice sheet occupying $-\infty < x < \infty$, $-\infty < y < \infty$, $0 < z < h$ floating on inviscid, irrotational water of depth H and density ρ (Fig. 2). Then, for no downward load, it is straightforward to derive a linearized surface-boundary condition for the ice sheet as follows (Fox and Squire, 1991b):

$$L\nabla^4\eta + \rho' h\eta_{tt} = -\rho\phi_t|_{z=0} - \rho g\eta \qquad (1)$$

where $\eta(x, y, t)$ represents a small vertical displacement of the ice sheet, and compressive stresses have been neglected. The effective flexural rigidity of the ice $L = Eh^3/12(1 - \nu^2)$, where E is the effective Young's modulus and ν is Poisson's ratio. The dispersion relation for uniform plane waves of wave number k and angular frequency ω travelling in the positive x-direction is found

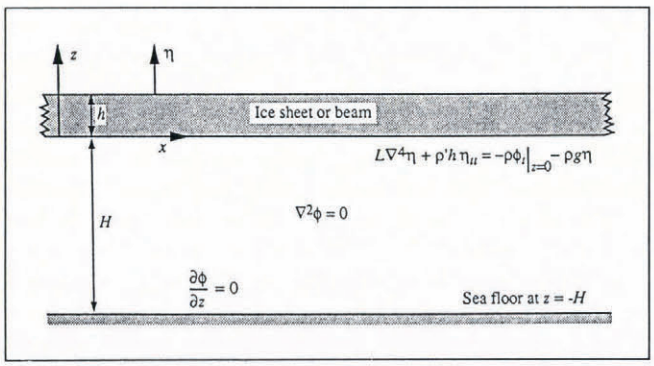

Fig. 2. Schematic showing ice sheet or beam of thickness h floating on water depth H.

https://doi.org/10.3189/S0022143000007462 Published online by Cambridge University Press

by assuming that the surface displacement η is everywhere proportional to $e^{i(kx-\omega t)}$. Then, using the kinematic boundary condition

$$\eta_t = \phi_{z|z=0} = k\tanh(kH)\phi|_{z=0} \qquad (2)$$

we substitute Equation (2) into Equation (1), to get

$$\omega^2 = \frac{Lk^5/\rho + gk}{kh' + \coth kH} \qquad (3)$$

where $h' = \rho' h/\rho$. This expression has been used many times to represent waves beneath a sea-ice plate (e.g. Squire, 1984a, b; Fox and Squire, 1990, 1991b; Davys and others, 1985; Wadhams, 1986), where the thickness h is small compared to the wavelength (i.e. $h \ll 2\pi/k$). In contrast to Equation (3), the dispersion relation most appropriate to a glacier tongue derives from consideration of a floating beam rather than a plate. The only difference, however, is that the flexural rigidity for a beam is defined by $L = EI$, where I is the moment of area of the beam about the xz-axis (Landau and Lifshitz, 1970, p. 89). In the case of a beam with a rectangular cross-section, which is basically a narrow plate, $L = Eh^3/12$. Then, the dispersion relation is identical to Equation (3), except for the factor $(1 - \nu^2)$ which appears in the denominator of L.

Surface strain

Anticipating the data analysis to follow, the strain amplitude at the ice surface must now be related to wave amplitude. For an infinite, homogeneous plate of thickness h bent infinitesimally, the strains are due to a simple change in geometry. Therefore the strains ϵ_{xx} and ϵ_{yy} in the x- and y-directions, respectively, are given by

$$\epsilon_{xx} = \frac{-h}{2}\frac{\partial^2\eta}{\partial x^2} \quad \text{and} \quad \epsilon_{yy} = \frac{-h}{2}\frac{\partial^2\eta}{\partial y^2}. \qquad (4)$$

For a wave of amplitude η_0 in the sea ice, the surface displacement will be $\eta(\mathbf{x}, t) = \eta_0 e^{i(\mathbf{k}.\mathbf{x}-\omega t)}$. Thus, writing the vector wave number $\mathbf{k} = (k\cos\theta, \sin\theta)$, where θ is the angle between $\mathbf{k}$ and the x axis, the surface-strain amplitudes for the sea ice are

$$\epsilon_{11} = \frac{h}{2}\eta_0 k^2\cos^2\theta \quad \text{and} \quad \epsilon_{22} = \frac{h}{2}\eta_0 k^2\sin^2\theta \qquad (5)$$

together with a shear-strain term ϵ_{12}.

For an ice tongue of finite width, there will also be a surface strain perpendicular to the direction of the major principal strain. This strain, i.e. the minor principal strain, was measured by Robinson and Haskell (1992). Assuming that the wave is propagating in the x-direction, i.e. along the beam, the principal strain ϵ_0 will also be in the x direction and

$$\epsilon_0 = \epsilon_{11} = \frac{h}{2}\eta_0 k^2 \quad \text{and} \quad \epsilon_{22} = -\nu\epsilon_0. \qquad (6)$$

An independent issue of particular concern to the EGT relates to the assumption in the derivation of Equation (4) that the neutral plane occurs half-way through the ice-tongue's thickness. This is clearly an approximation, as the ice properties are known to vary markedly throughout the thickness.

For both the sea ice and the EGT, we may write the displacement amplitude in terms of the principal surface strains using Expressions (5) and (6):

$$\eta_0 = \frac{2\epsilon_0}{hk^2} \qquad (7)$$

where

$$\epsilon_0 = \begin{cases} \epsilon_{11} + \epsilon_{22} & \text{for the sea ice} \\ \epsilon_{11} & \text{for the ice tongue.} \end{cases}$$

Angle θ may also be determined to the extent of four possibilities using orthogonal strain gauges located on the sea ice, since

$$\tan^2\theta = \frac{\epsilon_{22}}{\epsilon_{11}}. \qquad (8)$$

Note that, to find the displacement amplitude η_0, it is necessary to determine first the wave number k, which implies that the dispersion relation in Equation (3) must be used.

Energy density

The mean energy density is the sum of the energy density in the water column and that in the beam or plate. This will be used later to compare the energies of the surface gravity waves in the sea ice with those in the EGT. For a wave of amplitude η_0 and wave number k, the mean energy density E is given by

$$E = \frac{1}{2}\omega^2\eta_0^2\left(\rho' h + \frac{\rho}{k}\coth kH\right) \qquad (9)$$

or, in terms of the strain amplitude using Equation (7), by

$$E = \frac{2\omega^2\epsilon_0^2}{h^2k^4}\left(\rho' h + \frac{\rho}{k}\coth kH\right). \qquad (10)$$

THE WAVE DATA

The raw data comprise a series of surface-strain measurements made on the EGT and on the surrounding sea ice, using strain gauges sensitive to nano-strain. Four sets of strain measurements were made simultaneously at six locations for a period of 4 h each. Sampling was carried out at 2 Hz, so the Nyquist frequency was 1 Hz. The strain-data stream was first low-pass-analogue filtered at a cut-off frequency of approximately 0.5 Hz to remove any high frequencies, and was then recorded via a Maclab A-D system on to the hard disk of a Macintosh

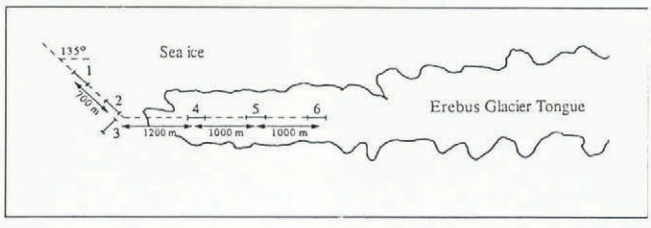

Fig. 3. Schematic showing positions and separation of the strain gauges on the ice tongue in relation to those on the sea ice. The numbers 1–6 attached to the strain gauges correspond to the channel numbers referred to in the text.

https://doi.org/10.3189/S0022143000007462 Published online by Cambridge University Press

computer. Four experiments were done on 19, 20, 21 and 22 November 1989. Three of the strain gauges were mounted on the EGT with their axes pointing along the tongue and three were located on the sea ice. The configuration is shown in Figure 3, with the distances between the instruments having been obtained by an accurate survey of the site. The numbers which distinguish the strain gauges in Figure 3 will be referred to as "channels" later in the text.

Pre-processing

The raw data are unsuitable for immediate spectral analysis for two reasons. First, there are long-term effects such as the action of the Sun on the ice and ice creep; both lead to a slow mean drift or trend in the strain readings which is not usually linear. This must be removed before spectral analysis to avoid contamination from irrelevant d.c. or near-d.c. energy. Secondly, there are steps in the data: to ensure that the instruments are always on scale and to maximize dynamic range, the strain gauges have a stepping motor that fires when the data drift out of range. The effect is to pull the data back on to scale and this appears as a near-instantaneous step from full scale to zero. The number of re-zeroes in a particular time series depends on the selected gain and on the degree to which the instruments are drifting due to natural effects. The steps are easily removed in the computer by setting to zero any changes greater than some threshold. Long-term trends in the data were removed by means of a Butterworth digital filter with a cut-off frequency of 0.0077 Hz (approximately 130 s) (Oppenhem and Schafer, 1975, chapter 5). Each data set was first low-pass filtered so that the drift could be examined without the distraction of oscillating waves. The drift was then subtracted from the original data. This method was chosen rather than direct application of a high-pass filter, so that the optimum cut-off frequency could be chosen by eye. Filtering was done twice, from left-to-right and from right-to-left, to avoid phase distortion. Once the data had been filtered, they were ready for spectral analysis. Sections of time series from the three strain gauges on the sea ice and the three on the ice tongue are shown in Figure 4a and b, respectively. The records suggest that the ice-tongue strain data were consistently of longer period than the data from the sea ice; counting cycles, the ice-tongue data appear to oscillate at around 50 s, whereas the principal period for the sea-ice data is about 12–13 s. The ice-tongue data are also of a consistently higher amplitude than the sea-ice data and less "noisy".

Some very narrow band-width, high-frequency noise was present in channels 4 and 6, and in some of the records from the strain gauges on the sea ice at precisely the same frequency. The noise is believed to be due to transmissions from the U.S. or N.Z. bases about 20 km down McMurdo Sound; the long lengths of unshielded wire used in recording the data acted as antennae. The effect may be associated with the pulse-repetition frequency of a typical radar. Fortunately, the noise was easily removed by notch-filtering the data.

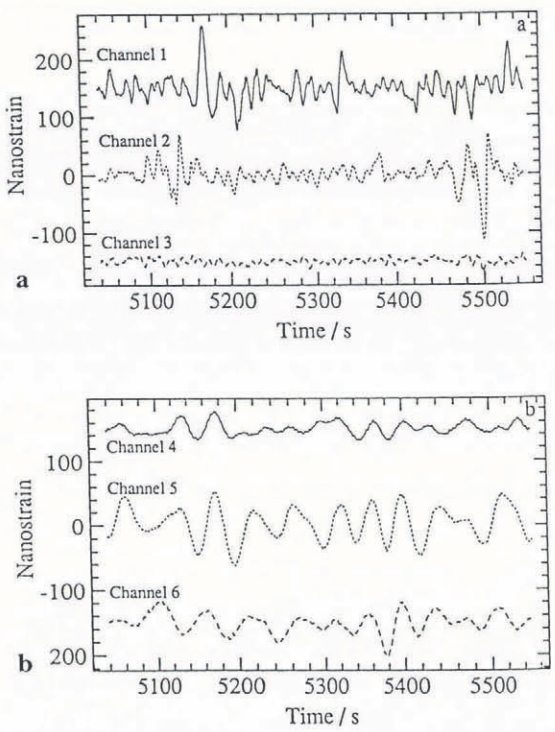

Fig. 4. Strain time series from (a) instruments on the sea ice and (b) instruments on the EGT. The channel numbers correspond to those of Figure 3.

Spectral analysis

Spectral analysis was performed on pairs of sequences using the Welch method of power-spectrum estimation. The two sequences of length 28 800 data points were divided into sub-sections of length 512 points, giving 112 degrees of freedom. Successive sub-sections were Hanning-windowed and then transformed with a 512-point fast Fourier-transform algorithm. With 112 degrees of freedom, the 95% confidence interval is approximately ±26% (Bendat and Piersol, 1986, p. 286). We denote the estimate of the auto-power spectrum of channels 1 and 2 by $G_1(f)$ and $G_2(f)$, respectively, where f is the frequency ($\omega = 2\pi f$) and their cross-power spectrum estimate by $G_{12}(f)$. An estimate of the transfer function $H(f)$ between sequences 1 and 2 is therefore

$$H(f) = \frac{G_{12}(f)}{G_1(f)} \tag{11}$$

(Bendat and Piersol, 1986, p. 166), so that the phase function $\beta(f) = \arg(H)$. The coherence function, defined

$$\gamma^2(f) = \frac{|G_{12}(f)|}{G_1(f)G_2(f)} \tag{12}$$

(Bendat and Piersol, 1986, p. 172), expresses the degree of statistical dependence between sequences.

A 95% confidence interval for the transfer function $H(f)$ may be found. For 112 degrees of freedom, the squared difference between our estimate and the true transfer function is less than $r^2(f)$, where

$$r^2(f) \approx 0.27 \frac{G_2(f)}{G_1(f)} (1 - \gamma^2(f)).$$

Thus, the error in the phase is $\Delta\beta(f) \approx \sin^{-1} |r(f)/H(f)|$ (Bendat and Piersol, 1986, p. 317).

https://doi.org/10.3189/S0022143000007462 Published online by Cambridge University Press

EGT power spectra

Power spectra derived from the channels on the ice tongue were consistent from day to day. The peak strains occurred at a frequency of 0.0195 ± 0.004 Hz (i.e. at about 50 s). The power spectrum of channel 4, located nearest the end of the ice tongue on 20 November 1989, is shown together with its confidence interval in Figure 5.

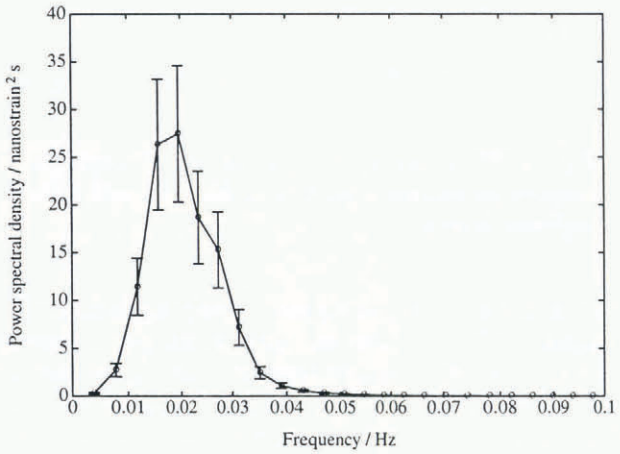

Fig. 5. Power spectrum (linear scale) of channel 4 together with its 95% confidence interval for 20 November.

Although a clear peak is apparent between about 1.8×10^{-2} Hz and 2.2×10^{-2} Hz (45–55 s), taking into account the resolution band width of 3.9×10^{-3} Hz, there is still a spread of significant energy from 0.01 to 0.035 Hz (28–100 s). Subsequently, we refer to the peak as being at 50 s, noting that there is some band width associated with this estimate. The power spectra for channels 4–6 on 19 November 1989 are shown in Figure 6. Channel 5 generally had larger power values than channels 4 and 6, and this is believed to be due to a difference in the geometry of the sites (calibration errors have been dismissed). If the strain gauge recorded as channel 5 were located, for instance, in an area where the EGT was thinner or above a heavily crevassed zone or even above an ice cave (of which there are many), then we would expect to see greater strain readings. This does not, of course, indicate that more energy is present. Unfortunately, the geometry of a site could not be ascertained as radio-echo sounding gear was not available. This highlights the problem of attempting to compare directly the amplitudes of time series recorded by different strain gauges; the power spectrum is not a measure of energy itself but of the square of strain amplitude, which is proportional to energy. Energy is also a function of frequency, ice thickness, etc. Thus, the constant of proportionality which relates the area beneath the power spectrum to energy varies between sites on the EGT.

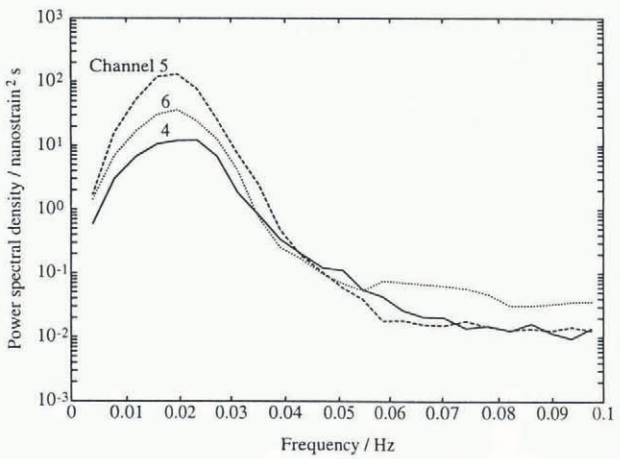

Fig. 6. Power spectra (logarithmic scale) for channels 4 (solid line), 5 (dashed line) and 6 (dotted line) on 19 November.

EGT transfer functions

Estimates of the transfer functions and coherence between channels on the EGT showed a number of salient features. Although there was some variation in the quality of the results obtained on each of the 4 d, the results were, in general, compatible. There was consistently a peak in the coherence of around 0.5. The most striking features were non-zero coherences in the range of frequencies from about 0.01 to 0.05 Hz, despite there being little energy present at the higher frequencies. This can be seen in Figure 7 which shows coherence for channels 4–5, 4–6 and 5–6 for data collected on 21 November. The broad span of non-zero coherence allows us to estimate the

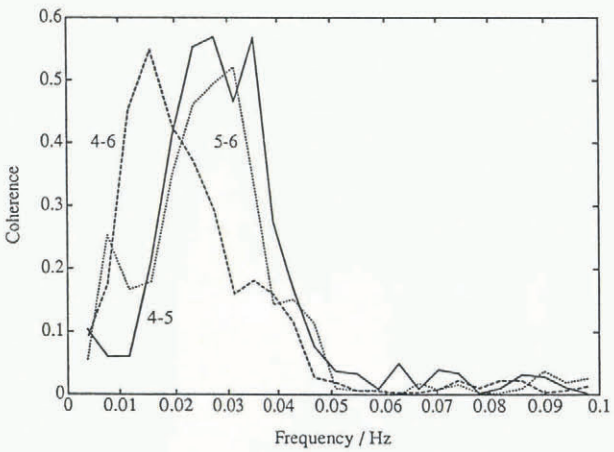

Fig. 7. Coherence functions for channels 4–5 (solid line), 4–6 (dashed line) and 5–6 (dotted line) for data collected on 21 November.

transfer function for a range of frequencies. Since the flexure detected by a strain gauge depends on the nature of a particular site as well as on the amplitude of the wave, the gain of the transfer function is of little interest and it is the phase function $\beta(f)$ which is of greatest value. The phase function between channels 4 and 5 is shown in Figure 8 together with its 95% confidence interval. This shows a number of features that were common to all of the phase functions, and the interpretation of this figure is central to the conclusions of this paper.

We consider the possibility that at any given frequency f_0 there are waves travelling in both directions, and reference our calculations to the first of two physically separated sites on the ice tongue. The strain at

https://doi.org/10.3189/S0022143000007462 Published online by Cambridge University Press

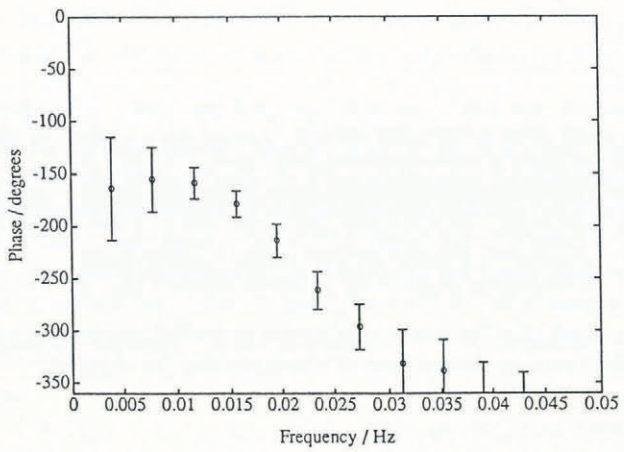

Fig. 8. Phase function between channels 4 and 6 for 19 November, with 95% confidence intervals.

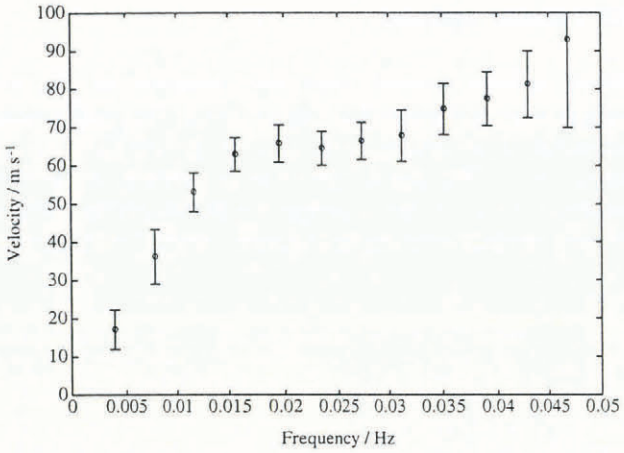

Fig. 9. Phase velocity c as a function of frequency, computed for channels 4 and 6 on 19 November with 95% confidence intervals.

the first site will be $(A + B)e^{i2\pi f_0 t}$, where A and B are the complex amplitudes of the waves travelling in each direction. The strain at the second site will be $R_{12}(Ae^{i\xi_0} + Be^{-i\xi_0})e^{i\omega_0 t}$ where R_{12} is the ratio of the amplitudes at either site, and ξ_0 is the phase difference between the sites at frequency f_0. The transfer function at f_0 is therefore given by

$$H(f_0) = R_{12}\left(\frac{Ae^{i\xi_0} + Be^{-i\xi_0}}{A+B}\right). \qquad (13)$$

In general, there is insufficient information to calculate the wave amplitudes A and B. However, we may consider two possibilities. The first occurs when the wave amplitudes have equal magnitude. Then, $B = Ae^{2i\alpha}$, where 2α is the arbitrary difference in the arguments of A and B, and the two waves interfere to create a standing pattern. The phase function in this case is given by

$$\beta(f_0) = \arg(H) = \arg\left(R_{12}\frac{\cos(\xi_0 - \alpha)}{\cos\alpha}\right) = 0° \text{ or } 180°. \qquad (14)$$

The second possibility is that the waves are travelling in only one direction. Then, $B = 0$, say, and the phase function becomes

$$\beta(f_0) = \arg(H) = \arg\left(R_{12}\frac{Ae^{i\xi_0}}{A}\right) = \xi_0. \qquad (15)$$

In this case, the phase difference between any two sites separated by a distance d for a wave propagating with velocity $c_0 (= 2_0/k)$ is

$$\beta(f_0) = \frac{2\pi f_0 d}{c_0}. \qquad (16)$$

Thus, if the wave is non-dispersive, the phase function will be linear in frequency f with a slope given by

$$\frac{d\beta}{df} = -\frac{2\pi d}{c_0}. \qquad (17)$$

We now return to Figure 8. The low-frequency limit of the phase function is approximately 180°, suggesting that at low frequencies the waves are travelling in both directions. From about 0.01 to 0.03 Hz, however, the phase function is approximately linear with a slope which gives a phase speed of $67\,m\,s^{-1}$ using Equation (17). Equation (16) may also be used to obtain a velocity estimate at each frequency (Fig. 9). This figure shows a distinct region of constant velocity of approximately $65\,m\,s^{-1}$. Noting that these two estimates are independent, this suggests that the band of waves centred around 50 s period is travelling with a phase velocity of approximately $65\,m\,s^{-1}$. The apparent decrease of phase speed to zero at low frequencies in Figure 8 is an artifact of applying Equation (16), which assumes the waves are travelling in only one direction, to frequencies at which waves are travelling in both directions.

Sea-ice power spectra

Strain measurements on the sea ice near to the EGT were inferior to those on the EGT itself. The strain gauges on the sea ice were not buried like those on the tongue and the measured strains were generally smaller (see Fig. 4). It proved possible to estimate power spectra for the sea-ice channels, but it was not possible to estimate transfer functions with any statistical accuracy. Sea-ice strain-power spectra (channels 1, 2 and 3) on 20 November are shown in Figure 10. Note that the power spectra for

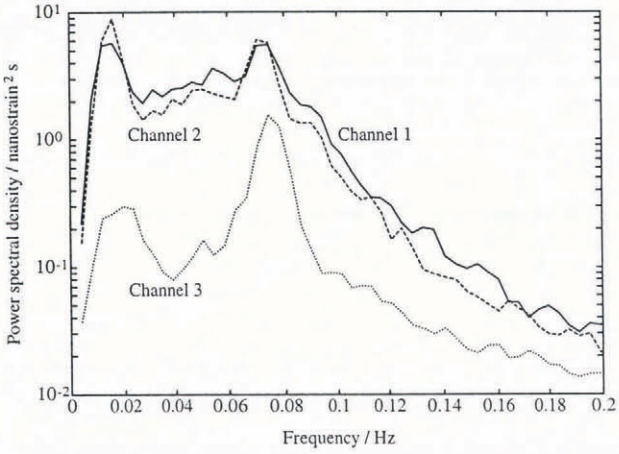

Fig. 10. Power spectra for sea ice on 20 November; channel 1 (solid line), channel 2 (dashed line) and channel 3 (dotted line).

https://doi.org/10.3189/S0022143000007462 Published online by Cambridge University Press

channels 1 and 2 are very similar, which is what would be expected from parallel but laterally displaced instruments. There are two peaks apparent at $0.15 \pm 1.95 \times 10^{-3}$ Hz (~67 s) and $0.075 \pm 1.95 \times 10^{-3}$ Hz (~13 s). Like the EGT, there is also significant energy present in the sea ice at a frequency of $0.02 \pm 1.95 \times 10^{-3}$ Hz (~50 s). The low values of coherence between the sea-ice channels makes transfer-function estimates unreliable, and thus phase speeds of the waves in the sea ice cannot be determined. It is assumed that the strains in the sea ice are due to flexural–gravity waves (Fox and Squire, 1991b) and are therefore governed by the dispersion Equation (3). The two strain gauges at right-angles do show a consistent phase change of zero, as expected.

The direction of the incoming flexural waves may be found from the two perpendicular strain gauges using Equation (8). This has been done for channels 2 and 3, which give a result of $\theta = 22° \pm 3°$ to 95% confidence. In choosing θ from its four possible values, we have assumed that the waves are propagating down McMurdo Sound, and have chosen an angle between the axis of strain gauge 2 and the axis of the EGT.

Dispersion: theory and experiment

Equation (3) describes the behaviour of flexural–gravity waves in the sea ice adequately but there are problems in applying it to the EGT over and above those discussed earlier. The ice tongue is quite irregular in shape and its cross-section is only approximated by a rectangle. Further, its cross-section changes along its length. Another problem is that the EGT is heavily crevassed and has many ice caves. These will reduce both its moment of area and the value of E. The value of the EGT's thickness h is only known approximately. The last radio-echo sounding was done about 4 years before the experiments reported in this paper (DeLisle and others, 1989), when it was found that the ice-tongue's thickness at approximately 1.5 and 3 km from the snout was 68.0 and 103.8 m, respectively. It is therefore clear that estimating the flexural rigidity L accurately is not possible. Finally, the water depth under the EGT is also not known accurately. Inevitably, then, values for the velocity of flexural waves in the EGT will be at best approximate.

It is now assumed that the most significant coupling between the flexural–gravity waves beneath the sea ice and those under the EGT occurs when the phase velocities, as given by Equation (3), are equal. We must allow for the fact that the velocity of the waves in the sea ice is at some angle ψ to the axis of the EGT. Thus, the phase-velocity component c_ψ of the waves down the EGT is related to the velocity in the sea ice (Fig. 11) by $c_\psi = c_{\text{sea ice}}/\cos\psi$. The theoretical dispersion curve for the sea ice with flexural rigidity $L = 11.3$ GN m, water density $\rho = 1025\,\text{kg m}^{-3}$, ice density $\rho' = 922.5\,\text{kg m}^{-3}$ and the corresponding curves for the EGT with various values of L ($L = 1 \times 10^5$, 2×10^5, 4×10^5 GN m, chosen because of our uncertainty about its true value), $h = 80$ m and the same densities as for the sea-ice plate are shown in Figure 12. All curves are for a water depth of 300 m. Sea-ice thickness is not critical for low-frequency waves where the dominant restoring force is gravity. The intersections of the dispersion curve for sea ice with those for the EGT certainly lie in the vicinity of the peak frequencies seen in the power spectra.

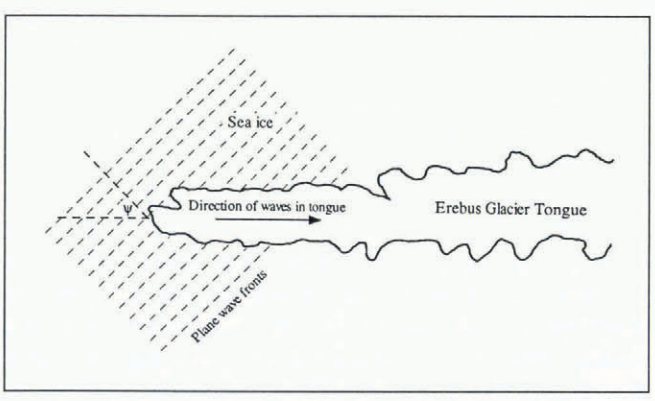

Fig. 11. Schematic showing the angle the waves are believed to be striking the EGT.

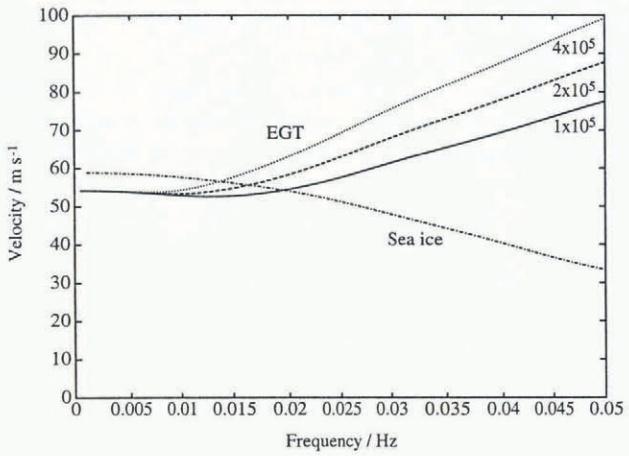

Fig. 12. Theoretical dispersion curves for the ice tongue with three values of flexural rigidity: $L = 1 \times 10^5$ GN m (solid line), 2×10^5 GN m (dashed line), 4×10^5 GN m (dotted line) and for the sea ice (chained line).

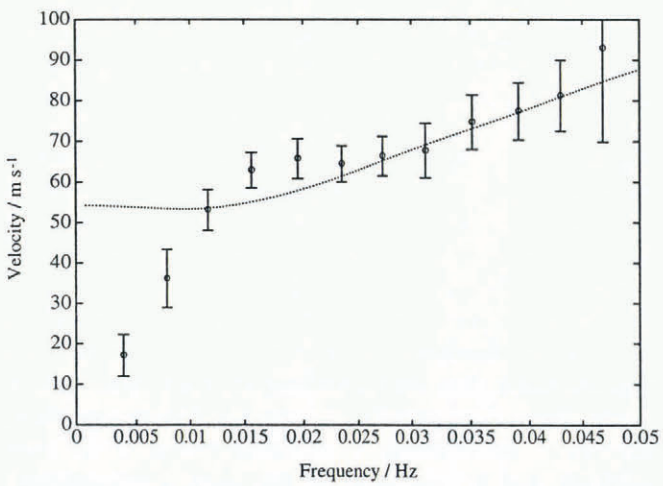

Fig. 13. The dispersion curve for the ice tongue ($L = 2 \times 10^5$ GN m) plotted together with phase velocities computed from channels 4–6, 19 November.

https://doi.org/10.3189/S0022143000007462 Published online by Cambridge University Press

Assuming $L = 2\,\mathrm{GN\,m}$, the dispersion curve for the EGT is plotted in Figure 13, together with phase velocities computed from the data. The figure shows a reasonable agreement between theory and the measured velocities except at low frequencies ($f \leq 0.01$ Hz), where we believe the velocity estimates are invalid as explained previously.

Energy density

If coupling is occurring between the waves under the sea ice and those under the EGT at 50 s, then it is of interest to obtain an order-of-magnitude estimate of the respective energy densities. To calculate this, the dispersion equation is required and it will be assumed that our theoretical dispersion Equation (3) is valid. To simplify the problem, we assume that all the energy in the EGT is at 50 s and that all the energy in the sea ice in the band 0.0156–0.0234 Hz is at 0.02 Hz (50 s).

To find the energy density, we use Equation (10). For the EGT, the square of the strain amplitude is calculated from the integral over all frequencies up to Nyquist. (In fact, this is no different from integrating over the first ten frequency bins, since there is virtually no energy at higher frequencies.) For the sea ice, the square amplitude of the strain at 50 s is found by integrating strain spectral-density values from 0.0156 to 0.0234 Hz, including the peak value at 0.0195 Hz. From Equation (7), the strains for channels 2 and 3 must be summed to get the principal strain amplitude in the sea ice. An average value for the strain amplitude of the sea ice is 8 nano-strain and for the EGT is 20 nano-strain. Choosing a phase speed $c = 65\,\mathrm{m\,s^{-1}}$ based on Figure 9, Equation (3) gives a wavelength of 3250 m. This gives a displacement amplitude for the EGT of $\eta_0 = 0.1$ mm, and for the sea ice of $\eta_0 = 1$ mm. Using Equation (10), the energy density of the flexural–gravity wave under 3 m thick sea ice is approximately $5 \times 10^{-3}\,\mathrm{J\,m^{-2}}$, whereas under the EGT, assuming a thickness of 80 m, it is about $5 \times 10^{-5}\,\mathrm{J\,m^{-2}}$. Thus, the wave-induced energy density of the EGT is about one-hundredth of that in the sea ice.

CONCLUSIONS

Like many geophysical measurements, there was undoubtedly significant noise with some unknown statistical distribution present in the strain measurements. This is demonstrated in the coherence function which reached a maximum of only 0.5, thereby indicating that only half the energy is accounted for by a linear-transfer function. However, the data sets used in the study were all very long and thus we have some confidence that statistically significant information has been extracted.

Our first conclusion is that, for the duration of the experiment, flexural waves of a period centred on approximately 50 s were travelling up the tongue with a phase speed of roughly $65\,\mathrm{m\,s^{-1}}$. At low frequencies, there appears to be evidence of standing waves, or at least evidence that a component of the wave is propagating down the EGT from the grounding line. In this context, it is worthwhile attempting to compute the eigenfrequencies corresponding to the normal flexural modes of oscillation of the ice tongue, invoking a simple fixed-free cantilever beam theory on a foundation which responds by buoyancy forces alone. Because the EGT tapers from its grounding line to snout and because of the many irregularities along its length, including variations in the bulk properties of the ice structure due to crevasses and ice caves, for example, the values obtained should be treated with caution. The first five non-dimensionalized modal wave numbers kl, where l is the length of the tongue, are 1.875, 4.694, 7.855, 10.996 and 14.137. These all correspond to eigenfrequencies of about 0.059 Hz (~17 s). Although kl is unaffected by the foundation on which the tongue rests, conversion to the eigenfrequencies at these wave numbers is dominated by buoyancy forces, and hence a full analysis which models the water beneath the ice tongue completely is probably necessary. Holdsworth and Glynn (1981) have used finite differences to solve the equations for a tapered beam on a fluid foundation. Their work shows that very long-period modes of standing oscillation are indeed possible in the tongue. Holdsworth (personal communication, 1993) also noted that a low-order harmonic may occur at about 50 s, and suggested that we may be observing a flexural wave propagating along the tongue which later is dissipated due to attenuation between the terminal area and the coastline, reflection at the coast and attenuation on its return journey. This is very plausible as the propagating strains detected are small.

It is also apparent that significant energy is present in the local sea ice, similarly in a band centred at approximately 50 s. If the EGT is radiating energy into the sea ice, then it would have to be taking energy input from some source other than the sea ice. Although there are candidates for this, such as the wind or tidal surges, this still poses a problem. Thus, if significant coupling between the EGT and the surrounding sea ice exists, it is most likely that it is the flexural–gravity waves in the sea ice which are driving the EGT. Indeed, the data suggest that the energy density at 50 s is much greater in the sea ice than in the EGT, which adds conviction to the notion that the waves in the sea ice are driving the EGT.

It has been assumed that optimum coupling occurs when the phase speed of the waves in the sea ice is equal to that in the EGT. This is obviously an approximation. More importantly, above 0.02 Hz, the phase speeds in the EGT and in the sea ice diverge, and coupling is unlikely. The sea-ice wave spectra peak between 59–77 s, yet the EGT spectra peak from 45 to 55 s. Why the EGT favours a band centred on 50 s period oscillation is unclear but it is probably associated with the geometry of the ice tongue.

Another difficult question to answer is the source of the peak in the sea-ice spectra at 67 s. A very long-period swell (infra-gravity wave) or a tidal seiche are both possibilities (Robinson and Haskell, 1992) but it is impossible to establish definitively the causal mechanism behind the long-period observations. Since the seiche fundamental in McMurdo Sound is not close to the observed period, non-linear energy-transfer processes would need to be invoked, or coupling at some harmonic; there are insufficient auxilliary data to proceed with either hypothesis. Infra-gravity waves of periods greater than 30 s, on the other hand, are certainly

an ubiquitous feature in pressure spectra taken in the deep ocean. Again, they are believed to originate from a non-linear transfer of energy from shorter-period waves, in this case surface gravity waves (Webb and others, 1991). Their presence in McMurdo Sound, which would appear very shallow to waves of this period, has not been established independently. The 67 s peak thus remains an open question.

The measurements in this experiment were made under conditions of solid-ice cover surrounding the EGT; conditions unlike those when the ice tongue calved when there was significant open water present. Therefore, it is difficult to draw conclusions about the mechanism of ice-tongue calving. What is apparent is that the EGT can be modelled as a beam floating on water. It is also apparent that the EGT is capable of being excited by water waves. Finally, it appears that there is some reflection of low-frequency waves at the grounding line to create standing waves. Further measurements are called for to reject or to confirm the standing-wave calving theory, and to qualify further the way in which the EGT is vibrating.

ACKNOWLEDGEMENTS

The authors are indebted to the New Zealand Foundation for Research, Science and Technology, the University of Otago, and the staff of the New Zealand Institute for Industrial Research and Development for their support. M.M. is a Ph.D. student supported on a Duffus Lubecki Postgraduate Scholarship in Applied Science. The authors are grateful to Dr G. Holdsworth of the Arctic Institute of North America for his constructive comments and suggestions.

REFERENCES

Bendat, J. S. and A. G. Piersol. 1986. *Random data: analysis and measurement procedures. Second edition.* New York, Wiley-Interscience.

Davys, J. W., R. J. Hosking and A. D. Sneyd. 1985. Waves due to a steadily moving source on a floating ice plate. *J. Fluid Mech.*, **158**, 269–287.

DeLisle, G., T. Chinn, W. Karlen and P. Winters. 1989. Radio echo-sounding of Erebus Glacier Tongue. *N.Z. Antarct. Rec.*, **9**(1), 15–30.

Fox, C. and V. A. Squire. 1990. Reflection and transmission characteristics at the edge of the shore fast sea ice. *J. Geophys. Res.*, **95**(C7), 11,629–11,639.

Fox, C. and V. A. Squire. 1991a. Coupling between the ocean and an ice shelf. *Ann. Glaciol.*, **15**, 101–108.

Fox, C. and V. A. Squire. 1991b. Strain in shore fast ice due to incoming ocean waves and swell. *J. Geophys. Res.*, **96**(C3), 4531–4547.

Goodman, D. J. and R. Holdsworth. 1978. Continuous surface strain measurements on sea ice and on Erebus Glacier Tongue, McMurdo Sound, Antarctica. *Antarct. J. U.S.*, **13**(4), 67–70.

Gui, E. H. and V. A. Squire. 1989. Random vibration of floating ice tongues. *Antarct. Sci.*, **1**(2), 157–163.

Holdsworth, G. 1969. Flexure of a floating ice tongue. *J. Glaciol.*, **8**(54), 385–397.

Holdsworth, G. 1974. Erebus Glacier Tongue, McMurdo Sound, Antarctica. *J. Glaciol.*, **13**(67), 27–35.

Holdsworth, G. 1982. Dynamics of Erebus Glacier Tongue. *Ann. Glaciol.*, **3**, 131–137.

Holdsworth, G. and J. E. Glynn. 1981. A mechanism for the formation of large icebergs. *J. Geophys. Res.*, **86**(C4), 3210–3222.

Holdsworth, G. and R. Holdsworth. 1978. Erebus Glacier Tongue movement. *Antarct. J. U.S.*, **13**(4), 61–63.

Landau, L. D. and E. M. Lifshitz. 1970. *Theory of elasticity. Second edition.* Oxford, Pergamon Press.

Oppenhem, A. V. and R. W. Schafer. 1975. *Digital signal processing.* Englewood Cliffs, NJ, Prentice Hall International.

Robinson, W. H. and T. G. Haskell. 1990. Calving of Erebus Glacier tongue. *Nature*, **346**(6285), 615–616.

Robinson, W. H. and T. G. Haskell. 1992. Travelling flexural waves in the Erebus Glacier Tongue, McMurdo Sound, Antarctica. *Cold Reg. Sci. Technol.*, **20**(3), 289–293.

Squire, V. A. 1984a. A theoretical, laboratory, and field study of ice-coupled waves. *J. Geophys. Res.*, **89**(C5), 8069–8079.

Squire, V. A. 1984b. On the critical angle for waves entering shore fast ice. *Cold Reg. Sci. Technol.*, **10**(1), 59–68.

Vinogradov, O. G. and G. Holdsworth. 1985. Oscillation of a floating glacier tongue. *Cold Reg. Sci. Technol.*, **10**(3), 263–271.

Wadhams, P. 1986. The seasonal ice zone. *In* Untersteiner, N., *ed. The geophysics of sea ice.* New York, Plenum Press, 825–991. (NATO ASI Ser. B, Physics, **146**.)

Webb, S.C., X. Zhang and W. Crawford. 1991. Infragravity waves in the deep ocean. *J. Geophys. Res.*, **96**(C2), 2723–2736.

The accuracy of references in the text and in this list is the responsibility of the authors, to whom queries should be addressed.

MS received 10 February 1993 and in revised form 1 April 1993